

Supporting Information for:

Body centered tetragonal nanoparticle superlattices

Leandro Missoni and Mario Tagliazucchi*

Instituto de Química Física de los Materiales, Medio Ambiente y Energía and Departamento de Química Inorgánica Analítica y Química Física, University of Buenos Aires, School of Sciences, Ciudad Universitaria, Pabellón 2, Ciudad Autónoma de Buenos Aires C1428EHA, Argentina

* email: mario@qi.fcen.uba.ar

1. Choice of calculation unit cell for NPSLs in bulk and on a substrate

The molecular theory calculations require to define a unit cell, which has periodic boundary conditions in the three dimensions (for bulk NPSLs) or in the two dimensions parallel to the substrate (for NPSL thin films). It is important to mention that the discretized lattice cells used to numerically solve the molecular theory have the same shape as the unit cell used in the calculation. In this way, during discretization, each unit cell is subdivided in an integer number of lattice cells in each direction (see Figure S2 in the Supporting Information of our previous work¹). Each lattice cell has a fixed volume equal to δ^3 , with $\delta = 0.15$ nm.

1.1. Bulk NPSLs

For bulk BCC, BCT and FCC cells, we used the two-NP unit cells shown in Figure 1a in the main text and Figure S1. The vectors that define the unit cell (see Figure S1) are:

$$\mathbf{v}_1 = (a, 0, 0) \quad (\text{S1})$$

$$\mathbf{v}_2 = (0, a, 0) \quad (\text{S2})$$

$$\mathbf{v}_3 = (0, 0, c) \quad (\text{S3})$$

where $c = a$ for BCC, $a < c < \sqrt{2}$ for BCT and $c = \sqrt{2}$ for FCC. The fractional positions of the two NPs in the unit cell are $\mathbf{f}_1 = (0, 0, 0)$ and $\mathbf{f}_2 = (\frac{1}{2}, \frac{1}{2}, \frac{1}{2})$.

For bulk NPSLs, the volume fraction of the solvent, ϕ_{sv} , determines the volume of the unit cell. The volume fraction of solvent is defined as:

$$\phi_{sv} = 1 - \phi_{NP} = 1 - \frac{N_{NP}(V_{core} + V_{ligand})}{V_{cell}} \quad (S4)$$

where ϕ_{NP} is the volume fraction of the NPs in the cell, $V_{cell} = a^2c$ is the volume of the unit cell, N_{NP} is the number of NPs per unit cell (two in this case), $V_{core} = (4/3)\pi R^3$ is the volume of the inorganic core and $V_{ligand} = 4\pi R^2 \sigma n_P v_P$ is the volume occupied by the ligand segments (σ , n_P and v_P are the ligand surface coverage, the number of segments per ligand and the volume of the segment, respectively). Therefore, the volume of the cell, V_{cell} , is fixed by ϕ_{sv} because V_{core} and V_{ligand} depend only on the properties of the NPs being modelled.

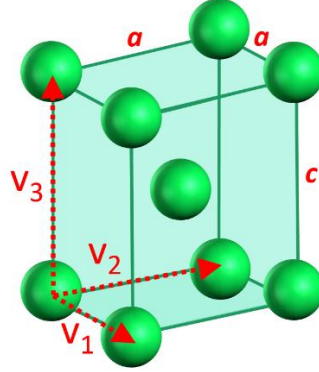


Figure S1. Scheme of a BCT unit cell showing the vectors \mathbf{v}_1 , \mathbf{v}_2 and \mathbf{v}_3 that define it. The system is periodic in the three dimensions.

1.2. NPSLs Films

The choice of the unit cell in thin NPSL films is more complex than for the bulk system. In NPSL films, periodic boundary conditions apply only in two directions.

1.2.1. $[110]_{sl}$ plane parallel to the substrate.

In this case, the $[110]_{sl}$ plane of the two-NP unit cell that forms the film (unit cell marked with red dashed lines in Figure S2a) should be parallel to the substrate. Note that the two-NP unit cell cannot be used as the unit cell for the film because it does not include the space between the NP layers and the substrate. Therefore, a different unit cell should be defined. Figure S2b shows in yellow the monoclinic unit cell employed in the calculations. This unit cell contains three NPs (one per NP layer). The vectors that define this cell are:

$$\mathbf{v}_1 = \frac{d_0}{\sqrt{\alpha^{-2} + 3 + 2\alpha^2}} (\alpha - \beta_1, \alpha - \beta_2, 0) \quad (S5)$$

$$\mathbf{v}_2 = \frac{d_0}{\sqrt{\alpha^{-2} + 3 + 2\alpha^2}} (\alpha - \beta_2, \alpha - \beta_1, 0) \quad (S6)$$

$$\mathbf{v}_3 = \left(\frac{1}{2\alpha}, \frac{1}{2\alpha}, 1 \right) d_{w-w} \quad (S7)$$

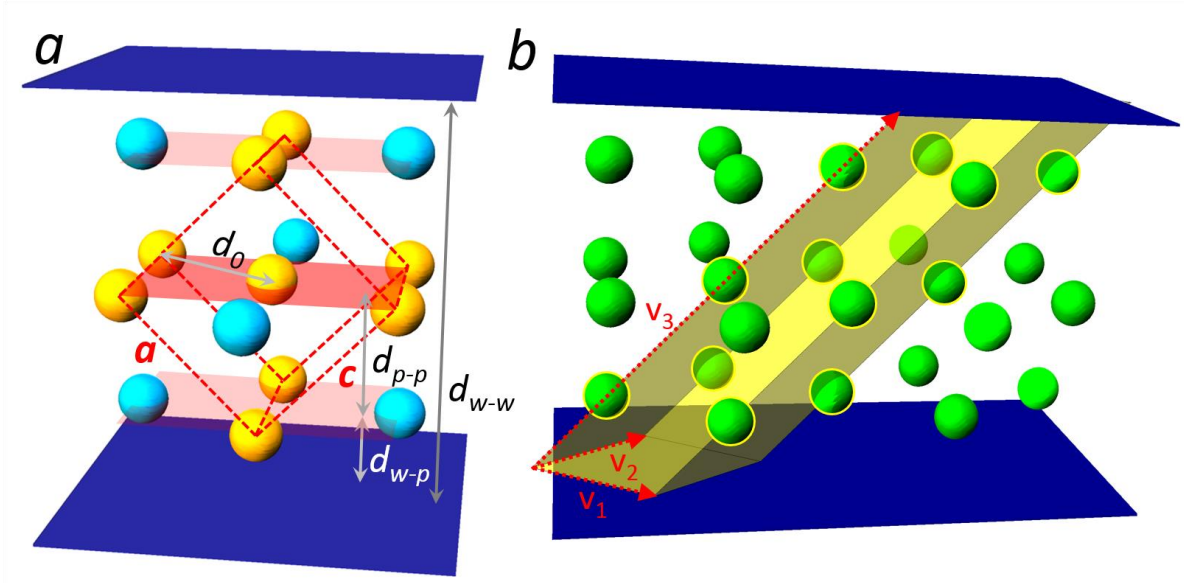


Figure S2. a. Scheme of a thin NPSL film having a BCC structure, three NP layers and its $[110]_{\text{SL}}$ plane aligned with the substrate. The two-NP unit cell is explicitly shown with red dashed lines. The distances d_0 , d_{p-p} , d_{w-p} and d_{w-w} correspond to the center-corner distance in the BCC unit cell, the separation between NP layers, the separation between the interfaces and their closest NP layer and the separation between interfaces, respectively. b. Scheme of the same system as in panel a, explicitly showing the monoclinic unit cell used in the molecular theory calculations for thin NPSL films and the vectors \mathbf{v}_1 , \mathbf{v}_2 and \mathbf{v}_3 that define it. The NPs with a yellow outline contribute a fraction of NP to the unit cell (the unit cell has three NPs in total). The system is periodic only in the directions given by \mathbf{v}_1 and \mathbf{v}_2 , which are parallel to the interfaces.

Note that \mathbf{v}_1 and \mathbf{v}_2 are parallel to the substrate. In Eqs. (S5)-(S7), d_0 is the distance between the central and corner NPs of the original two-NP unit cell (see Figure S2a), d_{w-w} is the separation between the two interfaces and α , β_1 and β_2 are auxiliary parameters that are related to the lattice parameters c and a of the original two-NP unit cell (shown in red dashed lines in Figure S2a) as:

$$\alpha = \frac{\sqrt{2}}{2} \frac{c}{a} \quad (\text{S8})$$

$$\beta_1 = \frac{1}{2} \left(-\alpha^{-1} + \sqrt{\alpha^{-2} + 2} \right) \quad (\text{S9})$$

$$\beta_2 = \frac{1}{2} \left(-\alpha^{-1} - \sqrt{\alpha^{-2} + 2} \right) \quad (\text{S10})$$

The parameter d_0 can also be related to a and c :

$$d_0 = \sqrt{\frac{1}{4}c^2 + \frac{1}{2}a^2} \quad (\text{S11})$$

The distance between planes of NPs, d_{p-p} can be calculated as:

$$d_{p-p} = \sqrt{\frac{1}{c^{-2} + a^{-2}}} \quad (\text{S12})$$

Finally, the distance between the interfaces and the layer of NPs closest to it, d_{w-p} , is:

$$d_{w-p} = \frac{d_{w-w} - (N_{\text{layer}} - 1)d_{p-p}}{2} \quad (\text{S13})$$

where N_{layer} is the number of NP layers in the film (in this case, $N_{\text{layer}} = 3$).

The fractional position of the NP j in the unit cell is:

$$\mathbf{f}_j = \left(0, 0, \frac{d_{w-p} + (j-1)d_{p-p}}{d_{w-w}} \right) \quad \text{for } 1 \leq j \leq N_{\text{layer}} \quad (\text{S14})$$

Finally, the volume fraction of the solvent in the cell, can be determined from Eq. (S4), using $N_{\text{NP}} = N_{\text{layer}} = 3$:

$$\phi_{sv} = 1 - \frac{N_{\text{layer}}(V_{\text{core}} + V_{\text{ligand}})}{V_{\text{cell}}} \quad (\text{S15})$$

The volume of the cell can be obtained from its definition $V_{\text{cell}} = \mathbf{v}_1 \cdot (\mathbf{v}_2 \times \mathbf{v}_3)$, where \mathbf{v}_1 , \mathbf{v}_2 and \mathbf{v}_3 are defined by Eqs. (S5)-(S7).

An analysis of the above equations shows that: i) ϕ_{sv} does is not completely fixed by the volume of the two-NP bulk cell (*i.e.*, the volume of the cell in red dashed lines in Figure S2a) because of the presence of the regions located between the interfaces and the closest NP layer. ii) Once the properties of the NPs and c/a (*i.e.*, the choice of BCC, BCT or FCC cell) are defined, the geometry of the system is determined only by two parameters, ϕ_{sv} and d_{w-w} . This result can be obtained with the following reasoning: given ϕ_{sv} , one can calculate V_{cell} from Eq. (S15). Now using the definition $V_{\text{cell}} = \mathbf{v}_1 \cdot (\mathbf{v}_2 \times \mathbf{v}_3)$ and the known values of d_{w-w} and c/a , one can use Eqs. (S5)-(S7) to obtain d_0 . Knowing d_0 and c/a allows to independently obtain a and c using Eq. (S11) and, then, d_{p-p} and d_{w-p} *via* Eqs. (S12) and (S13). In practice, we plotted our results in terms of ϕ_{sv} and d_{w-p}/d_{w-w} (Figure 2b in the main text) because these are the parameters that are invariant when the NPSL-film unit cells for BCC, BCT and FCC are discretized in the same number of lattice cells (we remind the reader that the discretized lattice cells have the same geometry as the unit cell).

1.2.1. [001]_{SL} plane parallel to the substrate.

The case where the [001]_{SL} plane is parallel to the substrate (Figure S3a) is much simpler than the previous one because the calculation cell is tetragonal and parallel to the substrate. The supercell considered in the calculation is shown in Figure S3b. Figure S3c shows the morphology diagram predicted for this orientation.

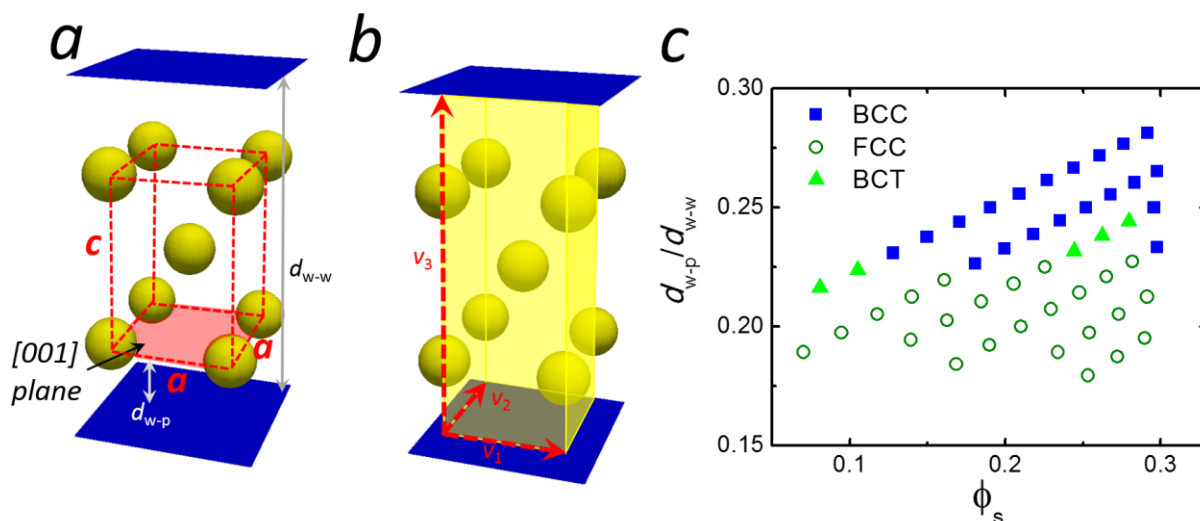


Figure S3. a. Scheme of a thin NPSL film having three NP layers and its $[001]_{\text{SL}}$ plane aligned with the substrate. The two-NP unit cell is explicitly shown with red dashed lines. The distances d_{w-p} and d_{w-w} correspond to the separation between the interfaces and their closest NP layer and the separation between interfaces, respectively. b. Scheme of the same system as in panel a, explicitly showing the tetragonal unit cell used in the molecular theory calculations for thin NPSL films and the vectors \mathbf{v}_1 , \mathbf{v}_2 and \mathbf{v}_3 that define it. The central NP contributes to one NP to the unit cell, while the other eight NPs contribute each with $\frac{1}{8}$ NP, thus the unit cell have three NPs in total. The system is periodic only in the directions given by \mathbf{v}_1 and \mathbf{v}_2 , which are parallel to the interfaces. c. Phase diagram for thin NPSL films with their $[001]_{\text{SL}}$ plane parallel to the substrate as a function of d_{w-p}/d_{w-w} and the volume fraction of solvent in the NPSL, ϕ_{sv} , for $\sigma = 4 \text{ ligands}\cdot\text{nm}^{-2}$, $n_p = 12 \text{ CH}_2/\text{ligand}$ and $R = 1 \text{ nm}$.

2. Free energy differences for bulk superlattices of spherical NPs in different conditions.

Figure S4 shows ΔF_{FCC} vs ϕ_{sv} plots for bulk superlattices of spherical NPs and different combinations of R (radius of NP core), n_p (number of CH_2 segments per ligand) and σ (density of ligands on the surface of the NPs). BCT phases are unstable in all conditions investigated.

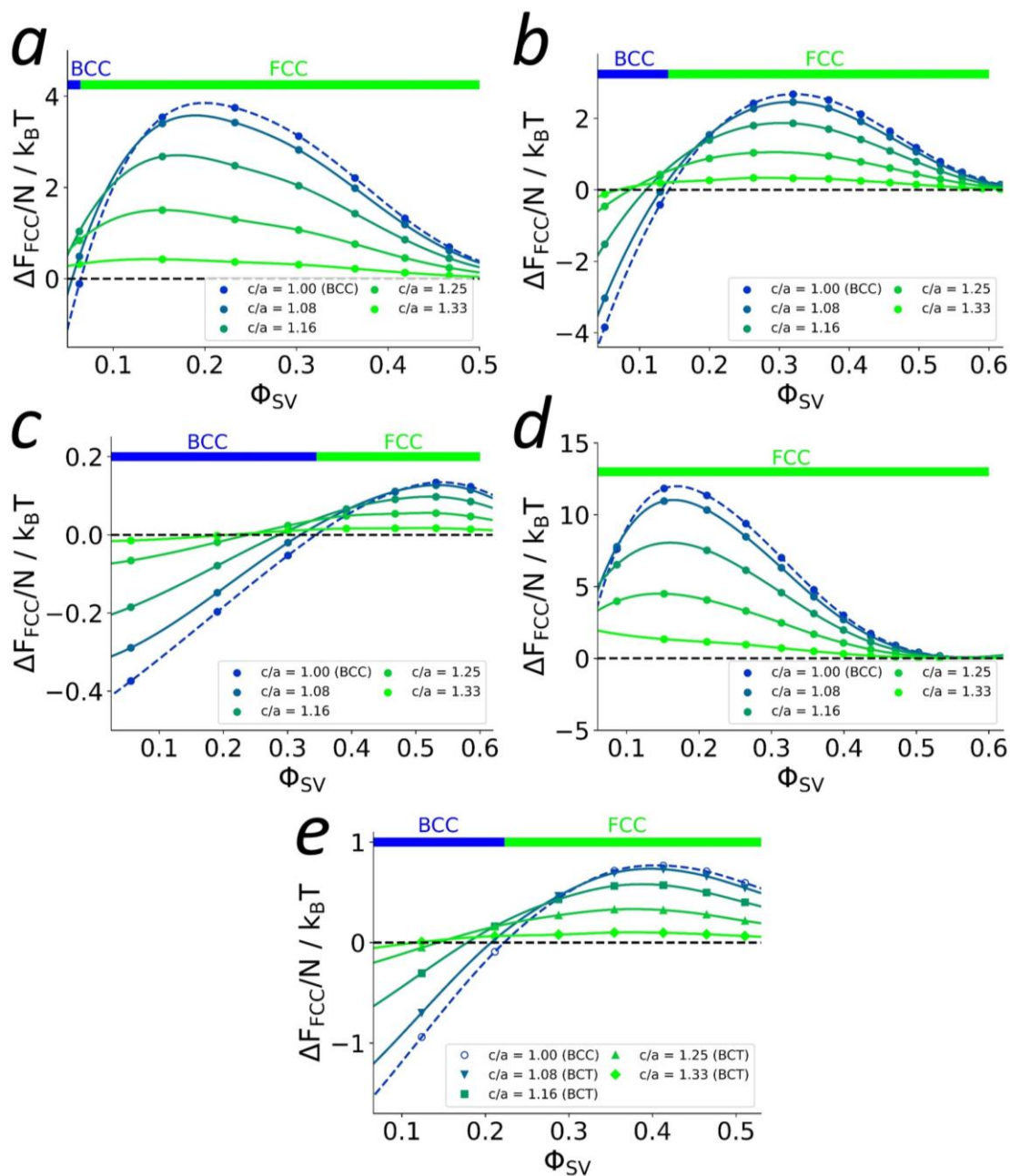


Figure S4: Free-energy differences between different structures and the FCC phase, ΔF_{FCC} for a bulk superlattice of spherical NPs as a function of the volume fraction of solvent in the lattice. Each plot corresponds to different calculation conditions: a. chain length, $n_p = 8 \text{ CH}_2/\text{ligand}$, b. $n_p = 16 \text{ CH}_2/\text{ligand}$. c. $R = 0,75 \text{ nm}$, d. $R = 2 \text{ nm}$, e. $\sigma = 2 \text{ ligands}\cdot\text{nm}^{-2}$. Other calculation parameters: $n_p = 12 \text{ CH}_2/\text{ligand}$ (c, d, e), $\sigma = 4 \text{ ligands}\cdot\text{nm}^{-2}$ (a, b, c, d), $R = 1.5 \text{ nm}$ (a, b, e).

3. Free energy differences for thin films of spherical NPs in different conditions.

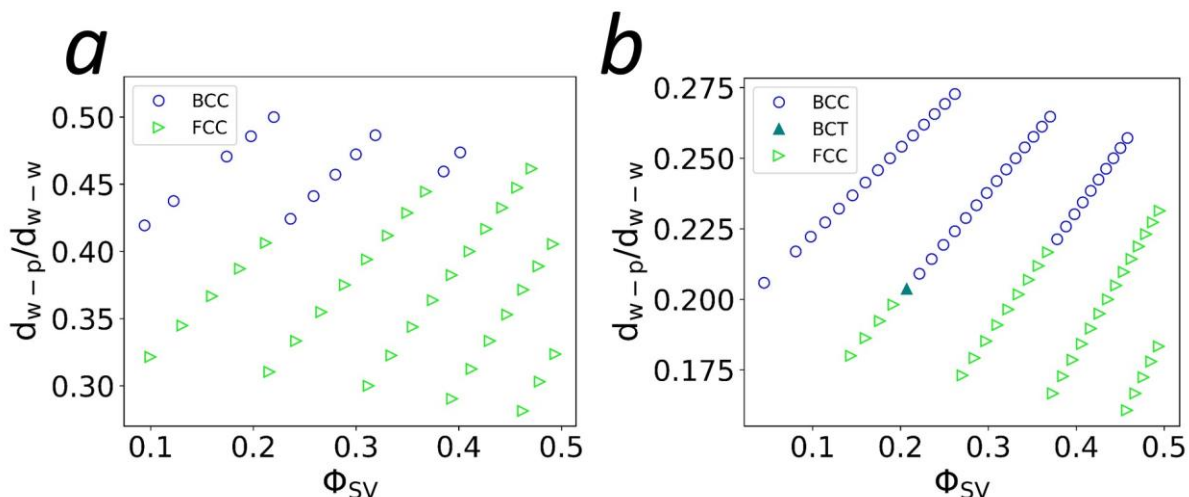


Figure S5: Phase diagram for thin NPSL films with their $[110]_{\text{SL}}$ plane parallel to the substrate as a function of d_{w-p}/d_{w-w} and the volume fraction of solvent in the NPSL, ϕ_{SV} , for different conditions. a. $\sigma = 4$ ligands $\cdot\text{nm}^{-2}$. b. $\sigma = 2$ ligands $\cdot\text{nm}^{-2}$. Other calculation parameters: $n_p = 12$ CH₂/ligand, $R = 1$ nm. The point reported for BCT in panel b corresponds to $c/a = 1.1$.

4. Free energy differences for bulk superlattices of spherical NPs calculated with the pairwise additive-approximation

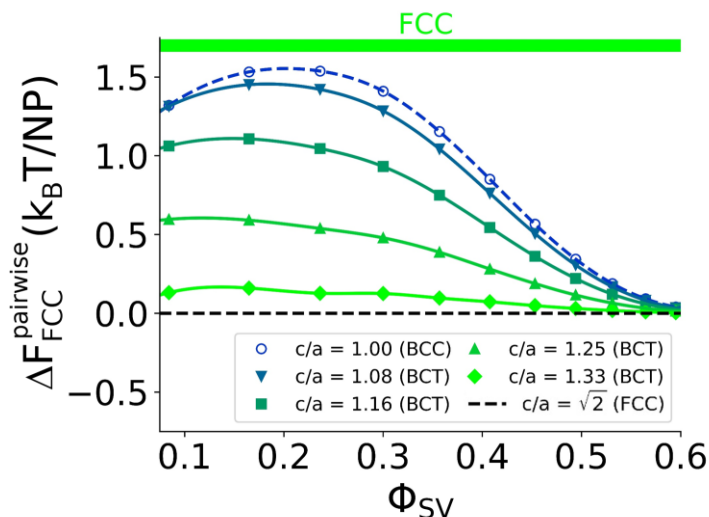


Figure S6: Free energy differences between different spherical NPSLs structures and FCC phase determined using the pairwise-additive approximation, $\Delta F_{\text{FCC}}^{\text{pairwise}}$, as a function of the volume fraction of solvent in the lattice. Same parameters as in Figure 1 in the main text: $n_p = 12$ CH₂/ligand, $\sigma = 4$ ligands $\cdot\text{nm}^{-2}$, $R = 1.5$ nm.

5. Analytical fitting formulas for pair potentials.

The pair potentials between NPs, F_{ij}^{pair} , can be trivially decomposed in the Hamaker attraction term and a repulsive term resulting from the overlap of ligand coronas:

$$\beta F_{ij}^{pair} = \beta F_{ij}^{pair,Ham} + \beta F_{ij}^{pair,rep} \quad (S16)$$

The Hamaker term is given by:

$$\beta F_{ij}^{pair,Ham} = -\frac{A}{6} \left[\frac{2R^2}{(d_{ij} + 2R)(d_{ij} - 2R)} + \frac{2R^2}{d_{ij}^2} + \ln \left(\frac{(d_{ij} + 2R)(d_{ij} - 2R)}{d_{ij}^2} \right) \right] \quad (S17)$$

where A is Hamaker's constant, R is the radius of the NP and d_{ij} is the distance between the centers of the NP cores. In practice, this term represents a very small contribution to F_{ij}^{pair} .

The repulsive component of F_{ij}^{pair} is obtained from molecular-theory calculations involving only two NPs at a core-core distance d_{ij} in a system without periodic boundary conditions. We found that the resulting potential can be fitted by an empirical analytical expression of the form:

$$\beta F_{ij}^{pair,rep} = A \exp(Bd_{ij} + Cd_{ij}^2 + Dd_{ij}^3 + \dots) \quad \text{for } d_{ij} > d_{\text{cut-off,min}} \quad (S18)$$

where in general it is enough to use up the quadratic term in d_{ij} inside the exponential, but in some cases the cubic term should be included to improve the fitting. Eq. (S18) has a minimum cut-off distance, $d_{\text{cut-off,min}}$, which is given by the minimum core-core distance for which we were able to converge the molecular-theory calculations for the two approaching NPs. The potential given by Eq. (S18) may be used in the future as an effective potential to describe ligand-mediated repulsions between NPs. Figure S7 shows an example of numerical results for $F_{ij}^{pair,rep}$ and the best fitting using Eq. (S18).

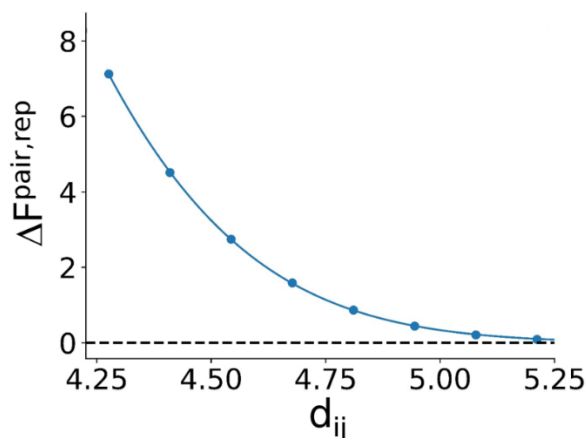


Figure S7: Repulsive part of the pairwise-interaction energy, $\Delta F_{\text{pair,rep}}$, as a function of the separation between particles, d_{ij} . The points show the predictions of the molecular theory, the solid line is the best fitting curve to the empirical equation $\Delta F_{\text{pair,rep}} = A \exp(Bd_{ij} + Cd_{ij}^2)$. Best fitting parameters: $A = 4.02 \times 10^{-5} k_B T$, $B = -8.84 \text{ nm}^{-1}$, $C = -1.41 \text{ nm}^{-2}$. The minimum cut-off distance is $d_{\text{cut-off,min}} = 4.28 \text{ nm}$. The calculations correspond to a spherical NPs with $n_p = 12 \text{ CH}_2/\text{ligand}$, $\sigma = 4 \text{ ligands} \cdot \text{nm}^2$, $R = 1.5 \text{ nm}$.

6. Distances between opposing facets in TO-NPSLs.

In this section we will consider the distances between opposing facets of TO-NPs along the $\perp[111]_{\text{SL}}$ and the $\perp[100]_{\text{SL}}$ directions. In general, we can write:

$$D_{\text{surf-surf}} = D_{\text{center-center}} - 2d_{\text{center-surf}} \quad (\text{S19})$$

where $D_{\text{surf-surf}}$ is the distance between the surfaces of two involved NPs (*e.g.*, the surfaces of the opposing squares in the $\perp[100]_{\text{SL}}$ direction or the opposing hexagons in the $\perp[111]_{\text{SL}}$ direction, see Figure 3b in the main text), $D_{\text{center-center}}$ is the distance between the centers of those two NPs, and $d_{\text{center-surf}}$ is the distance between the center of a NP and its surface in the direction that connects the two NPs. In the case of opposing square facets (interaction along the $\perp[100]_{\text{SL}}$ direction), Figure 3a in the main text clearly shows that $d_{\text{center-surf}} = L_{\text{cube}}/2$, which takes values between 1.3 and 1.6 nm for the system studied in Figure 3d in the main text. On the other hand, for opposing hexagonal facets (interaction along the $\perp[111]_{\text{SL}}$ direction), the calculation is more complex because the vector that connects the centers of the NPs is perpendicular to the hexagonal facets only for the BCC cell, but not for BCT and FCC. However, the deviation from perpendicularity in the latter cases is not too large, so we will approximately consider that the vector connecting the two particles always goes through the center of the hexagons. Therefore, $d_{\text{center-surf}}$ corresponds to the inner radius of the octahedron that gives origin to the TO (*i.e.*, $d_{\text{center-surf}}$ will be the radius of a sphere that is tangent to the hexagonal facets of the TO). This approximation results in $d_{\text{center-surf}} = (3^{1/2}/6)L_{\text{octa}} = 1.3$ nm.

In the example of a FCC cell analyzed in the main text, each NP has 12 near neighbors located at the same distance $D_{\text{center-center}}$. Therefore, according to the calculations in the previous paragraph, the separation between the surfaces of the opposing squares for NPs interacting in the $\perp[100]_{\text{SL}}$ direction is 0 to 0.6 nm smaller (for $L_{\text{cube}} = 2.6$ and 3.2 nm, respectively) than the separation between the hexagonal facets of NPs interacting along the $[111]_{\text{SL}}$ direction.

References

- (1) Missoni, L. L.; Tagliazucchi, M. The Phase Behavior of Nanoparticle Superlattices in the Presence of a Solvent. *ACS nano* **2020**, *14* (5), 5649–5658.